

Theoretical confirmation of a high-pressure rhombohedral phase in vanadium metal

Byeongchan Lee,* Robert E. Rudd, John E. Klepeis, Per Söderlind, and Alexander Landa
Lawrence Livermore National Laboratory, University of California, Livermore, California 94551, USA

(Received 18 April 2007; published 18 May 2007)

Recent diamond-anvil-cell (DAC) experiments revealed a new phase in vanadium metal at high pressure. Here we present results from first-principles electronic-structure calculations confirming the existence of this phase. The structure corresponds to a rhombohedral distortion of the bcc ambient-pressure phase. The calculated transition pressure (0.84 Mbar) and density compare reasonably with the measured data. Interestingly, a reentrant bcc phase is discovered at ultrahigh pressures above 2.8 Mbar, close to the limit of DAC experimental capabilities. We show, extending prior work, that the phase transitions in vanadium are driven by subtle electronic-structure effects.

DOI: [10.1103/PhysRevB.75.180101](https://doi.org/10.1103/PhysRevB.75.180101)

PACS number(s): 62.50.+p, 61.50.Ks

It was proposed in theoretical studies that vanadium should become mechanically unstable in its ground-state bcc phase at sufficiently high pressure.^{1,2} Suzuki and Otani¹ performed calculations of the lattice dynamics of vanadium in the pressure range up to 1.5 Mbar. They found that a dip (Kohn anomaly) in the transverse acoustic (TA) phonon branch along the $[\xi 00]$ direction near $\xi_0=1/4$ shows a dramatic softening under pressure and eventually becomes imaginary at ~ 1.3 Mbar, indicating the possibility of a structural phase transition. Later Landa *et al.*² suggested that the Kohn anomaly in the TA phonon at $\xi_0=1/4$ was a consequence of intraband Fermi surface (FS) nesting. It is often the case that phenomena of this type precede a martensitic phase transformation. In the case of vanadium it was found that premartensitic softening of the TA phonon mode under compression triggers a decrease of the shear elastic constant C_{44} , which becomes negative at megabar pressures.² It was also found that the softening (decrease) in C_{44} develops up to the point when the nesting vector ($2\xi_0$), which spans two parallel pieces of the so-called “jungle-gym” hole tube of vanadium, goes to zero.² In other words, the minimum in C_{44} coincides with an electronic topological transition (ETT) in which a neck appears between two FS sheets. The electronic structure calculations within density functional theory (DFT) predicted and explained the negative C_{44} elastic constant at megabar pressures,² but a specific crystal structure resulting from this instability was not proposed.

The earlier theoretical work of Landa *et al.*² motivated a renewed interest in vanadium, and diamond-anvil cell (DAC) measurements³ recently confirmed that vanadium is indeed unstable in its cubic phase. Ding *et al.*³ found that, at pressures starting in the 0.6–0.7-Mbar range, a rhombohedral transition occurs corresponding to an increase in the angle α between the primitive unit-cell vectors spanning the bcc crystal. They observed the rhombohedral phase to be stable up to the highest pressure studied, 1.55 Mbar. However, an earlier DAC study under hydrostatic conditions reported that the bcc cubic phase remained stable up to 1.54 Mbar.⁴ It is thus of significant importance to distinguish between these very different experimental results by carrying out accurate electronic-structure calculations to address the existence of a bcc-to-rhombohedral transition.

In this article we address the phase stability of vanadium

metal up to and beyond the heretofore measured pressure. Specifically, we apply DFT in combination with a gradient-corrected exchange and correlation energy functional⁵ as implemented in the Vienna *ab initio* simulation package (VASP) code along with the projector augmented-wave (PAW) method⁶ and standard computational parameters.⁷ Because the instability is believed to be linked to a shear distortion defined by C_{44} , we apply a generalization of the conventional volume-preserving monoclinic distortion used by Landa *et al.*:^{2,8}

$$T(\delta) = \begin{pmatrix} 1 & \delta & 0 \\ \delta & 1 & 0 \\ 0 & 0 & \frac{1}{1-\delta^2} \end{pmatrix}, \quad (1)$$

where $T(\delta)$ is the transformation matrix or deformation gradient and δ parametrizes the distortion. The limitation of this particular strain path is that it corresponds to monoclinic symmetry (prismatic shear deformation) and does not allow for a rhombohedral distortion. Instead, the rhombohedral lattice system is obtained by applying a strain in the threefold direction and determined by a single lattice constant and an angle α made by any two axis vectors. The volume-conserving bcc-to-rhombohedral transformation matrix is defined as

$$T(\delta) = \begin{pmatrix} k & \delta & \delta \\ \delta & k & \delta \\ \delta & \delta & k \end{pmatrix}, \quad (2)$$

where k is determined from the real positive solution of $\det(T)=1$ to ensure a volume-conserving transformation. The small displacement δ represents the amount of rhombohedral deformation of the bcc crystal: a positive δ corresponds to a decrease in α from the bcc value of $\alpha_0=109.47^\circ$. As we are exploring relatively small distortions, the normalizing factor k is always close to 1.

The volume-conserving rhombohedral transformation described in Eq. (2) does not result in strictly constant pressure. The total energy along the deformation path can be corrected from an internal energy to an enthalpy in order to investigate phase stability at constant pressure. For small δ , the enthalpy

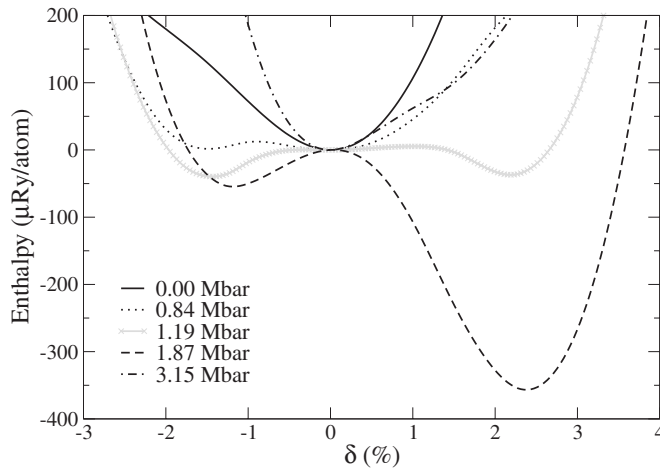


FIG. 1. Enthalpy as a function of the rhombohedral deformation parameter δ . The different curves correspond to the pressures indicated in the legend.

at pressure $P_0 = P(\delta=0, V_0)$ may be calculated to a good approximation from the internal energy using the formula

$$H(\delta, P_0) \approx U(\delta, V_0) + P_0 V_0 - \frac{1}{2B(\delta, V_0)} \Delta P(\delta, V_0)^2 V_0, \quad (3)$$

where $\Delta P(\delta, V_0)$ is the pressure change at the given volume V_0 due to the rhombohedral transformation δ —i.e., $P(\delta, V_0) - P_0$. B is the bulk modulus at the given volume. The internal energy differences are small, but nonetheless it turns out that the correction in Eq. (3) is not significant, and thus the internal energy is sufficient to study phase stability.

In Fig. 1 we show the calculated enthalpies as a function of the rhombohedral distortion for various pressures. At ~ 0.73 Mbar a metastable rhombohedral structure develops and becomes the ground state at ~ 0.84 Mbar. The negative sign of the strain parameter δ reflects an increase in the angle α relative to the cubic structure, to a value of 110.25° . Between 1.03 Mbar and 1.12 Mbar another rhombohedral local minimum with a positive value of δ appears, resulting in three local minima including the bcc structure. At this point the curvature of the strain energy curve is still positive for bcc ($\delta=0$), so it remains mechanically stable. The fact that the bcc structure becomes thermodynamically unstable but remains mechanically stable is not observed in the case of the monoclinic shear deformation given in Eq. (1), for which the strain-energy curve is essentially symmetric for small strains. At roughly 1.19 Mbar the ground state switches to the rhombohedral structure with positive δ , but the first (negative δ) rhombohedral structure remains metastable to a pressure of ~ 2.49 Mbar. The rhombohedral structure with positive δ attains its greatest stability at 1.87 Mbar, with $\alpha = 108.14^\circ$. As the pressure is further increased the ground state finally reverts back to the bcc structure at ~ 2.8 Mbar, and at 3.15 Mbar the bcc structure becomes the only mechanically and thermodynamically stable structure. It is interesting to note that there are two competing rhombohedral structures with opposite sign for the change in α .

We have examined the possibility that the true ground state might further break the rhombohedral symmetry. For example, a structure that is a combination of the monoclinic and rhombohedral shears could have even lower energy. In order to address this issue we have generated a full three-dimensional energy landscape using a multivariate fit obtained from calculations for the two shear deformations. The resulting energy landscape confirms that the rhombohedral structure is the true ground state and the minimum energy along the monoclinic deformation path (1) corresponds in higher-dimensional shear space to a saddle point between two rhombohedral local minima.

With regard to the shear instability, we find that the bcc structure is mechanically unstable with a negative C_{44} from 1.41 to 2.49 Mbar, in good agreement with the results of Landa *et al.*² The fact that the pressure range of the shear instability is completely contained within the range of the stable rhombohedral structure is suggestive of subtle electronic effects beyond the monoclinic C_{44} shear instability itself. Even at ambient pressure, there is a noticeable feature in the enthalpy curve for δ of -1.5% to -2% . This feature persists over a broad pressure range, indicating that an abrupt change in the Fermi-surface topology as a function of pressure (Lifshitz transition⁹) is not the driving force. The rhombohedral distortion produces an energetically favorable change in the electronic structure, but this change is smaller than the overall increase in energy at ambient pressure due to elasticity. However, the relative magnitude of the energy lowering increases with pressure as the shear softening further develops and finally leads to a new ground state. When C_{44} is negative there is a combined effect of rhombohedral stabilization and shear instability in the bcc structure, leading to the prominent rhombohedral phase. Thus it is natural to see the stable rhombohedral phase before entering and after exiting the region of bcc shear instability as pressure is increased.

At the transition pressure, the enthalpy curves in Fig. 1 exhibit a barrier between the bcc and rhombohedral phases, indicating a first-order transition at zero temperature. Due to the very small enthalpy differences, however, it is difficult to conclude from the DFT calculations whether the transition should be observed experimentally as first order or second order. At room temperature, thermal fluctuations are larger than the latent heat of transformation, and it is natural to expect the transition to be second order. For example, when the rhombohedral phase becomes the ground state at roughly 0.84 Mbar, the energy barrier between the emerging rhombohedral phase and the bcc phase is very small as can be seen in Fig. 1. The resulting flat enthalpy basin, as it is explored by thermal fluctuations, significantly weakens the first-order nature evident at zero temperature. The result is that the fine structure of the enthalpy curve is washed out by thermal fluctuations and only the overall anharmonicity is probed so that the phase change appears gradually, as reported in recent experimental work.³ The theoretical order parameter ($Q = \alpha/\alpha_0 - 1$) at zero temperature is plotted in Fig. 2; “bcc” represents the ambient-pressure ground state, and “stable structure” stands for a mechanically stable yet thermodynamically unfavorable local minimum against formation of the “ground state.” Immediately evident in this

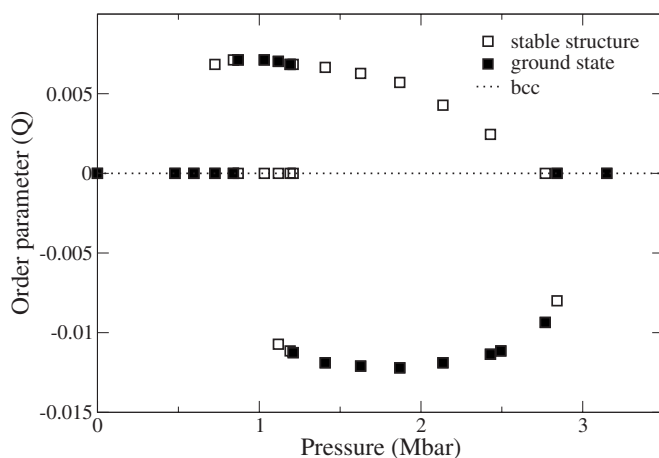


FIG. 2. The order parameter for mechanically stable structures as a function of pressure at zero temperature. The order parameter is defined as $Q = \alpha/\alpha_0 - 1$, where $\alpha_0 = 109.47^\circ$ is the axis angle of the bcc structure.

plot is an abrupt (first-order) change in the order parameter. This abrupt change might not be observed in experiments at finite temperature for the reasons just discussed, and indeed the Ding *et al.*³ observed the order parameter to grow continuously from zero as the square root of the pressure beyond the transition pressure, $Q \sim \sqrt{P - P_c}$.

The theoretical transition pressures are obtained from the calculated response to hydrostatic compression at zero temperature. In Fig. 3 we show our calculated equation of state together with the room-temperature DAC data of Ding *et al.*³ The experimental data points were obtained from nonhydrostatic (NH) and quasihydrostatic (QH) pressures, where the open (solid) symbols refer to the bcc (rhombohedral) phase. The NH data were obtained from a vanadium sample loaded in the DAC chamber without a pressure medium, whereas for the QH data helium was used for this purpose. The QH data are noticeably different than the NH data and in better agreement with the calculations, as expected, since the calculations correspond to perfectly hydrostatic compression.

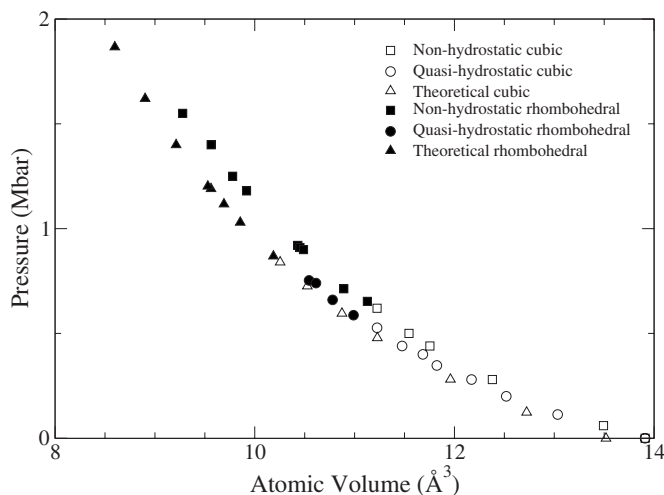


FIG. 3. Experimental data from Ding *et al.* (Ref. 3) together with the present calculations.

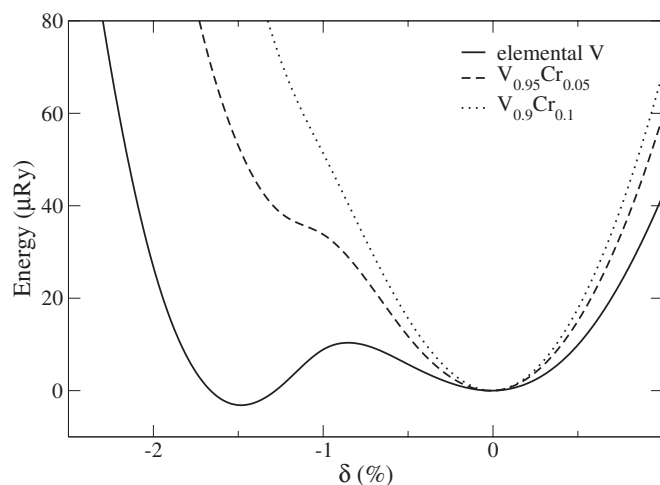


FIG. 4. Calculations showing the effect on the energy of including Cr within the virtual crystal approximation at $V = 9.86 \text{ \AA}^3$.

For the QH measurements the bcc-to-rhombohedral phase transition takes place at a pressure of 0.59 Mbar and an atomic volume of 10.99 \AA^3 . These results compare relatively well with the calculated transition pressure of 0.84 Mbar and atomic volume of 10.25 \AA^3 . We note that the second rhombohedral structure with a positive value of δ (negative order parameter) becomes the ground state at a slightly lower pressure than the highest QH pressure studied in the DAC experiments. This second rhombohedral structure has not been seen in experiment. The calculated transition pressure is sensitive to the computational details, with the transition pressure from fully converged calculations varying by ~ 200 kbar; e.g., all-electron calculations,¹⁰ not relying on the pseudopotential assumption, predict the transition at 0.60 Mbar (10.78 \AA^3), in near perfect agreement with the experimental data.

The presence of defects or impurities in the experimental samples could lead to differences between theory and experiment. Landa *et al.*² have shown that alloying with a small concentration of niobium removes the C_{44} instability in bcc vanadium. In addition, hydrogen and oxygen impurities commonly occur in vanadium and are known to influence the elastic properties.¹¹ Introducing impurities will smear out the sharp Fermi-surface features that give rise to the elastic and structural instabilities. Similarly, we find that smearing out the electronic density-of-states (DOS) using a Fermi-Dirac distribution and an electron temperature of 2000–3000 K also removes the shear instability.¹² The pressure dependence of the instability occurs because the s -like bands move higher and the d -like bands move lower in energy relative to the Fermi level with increasing compression (s - d transition¹³), thus altering the nature of the Fermi surface and restricting the instability to a particular pressure window. As we have already indicated above, the fact that the instability exists over a broad range of pressures argues against a Lifshitz transition.⁹ We can further confirm the Fermi-surface-related driving force by artificially shifting the Fermi level and thereby removing the relevant features from the Fermi surface at a fixed volume. This shift can easily be accomplished by essentially doping the vanadium with chromium,

which has one extra valence electron, and applying the virtual crystal approximation (VCA) in which the vanadium atoms are replaced by “average” atoms whose atomic number is a concentration-weighted average of those of the constituents. Although the details of change in the system volume and energy due to chromium inclusion are not relevant to the Fermi-surface effects or readily available within the VCA, such information would be useful for a better understanding of alloy materials and can be obtained with extensive calculations including heat of mixing. In Fig. 4 we see that the energy as a function of the rhombohedral distortion for $V_{0.95}Cr_{0.05}$ no longer exhibits an instability while all evidence of the instability is essentially gone in the case of the curve corresponding to $V_{0.9}Cr_{0.1}$. These results strongly support the existence of a Fermi-surface-related driving force. Finally, the two remaining column-VB transition metals, niobium and tantalum, also exhibit noticeable C_{44} elastic softening as a function of pressure,^{2,12} although both remain mechanically stable. The electronic structures of niobium and tantalum are very similar to that of vanadium except that the $3d$ band is replaced by the $4d$ and $5d$ bands, respectively. It

is also interesting that a differently deformed structure has been proposed as a metastable phase of vanadium at $P \sim 0$.¹⁴

We have confirmed the existence of a rhombohedral phase in vanadium metal as recently suggested by high-pressure DAC experiments.³ The calculated stability of this phase ranges from about 0.84 Mbar up to a predicted 2.8 Mbar. The primary reason for the instability is pressure-induced Fermi-surface effects that have been discussed previously.² As a function of compression an s - d transition shifts the Fermi level through and then beyond the region of electronic instability, thus destabilizing and then restoring the bcc phase in vanadium. This example of a cubic \rightarrow distorted phase \rightarrow cubic series of phase transitions is uncommon in an elemental metal but the Fermi-surface-related driving force and the corresponding elastic softening as a function of pressure may occur much more generally.

This work was performed under the auspices of the U.S. DOE by the University of California, LLNL, under Contract No. W-7405-Eng-48.

*Electronic address: airbc@llnl.gov

¹N. Suzuki and M. Otani, *J. Phys.: Condens. Matter* **14**, 10869 (2002).

²A. Landa, J. Klepeis, P. Söderlind, I. Naumov, L. Vitos, and A. Ruban, *J. Phys.: Condens. Matter* **18**, 5079 (2006); A. Landa, J. Klepeis, P. Söderlind, I. Naumov, O. Velikokhatnyi, L. Vitos, and A. Ruban, *J. Phys. Chem. Solids* **67**, 2056 (2006).

³Y. Ding, R. Ahuja, J. Shu, P. Chow, W. Luo, and H.-K. Mao, *Phys. Rev. Lett.* **98**, 085502 (2007).

⁴K. Takemura, in *Science and Technology of High Pressure*, Proceedings of AIRAPT-17, Hawaii, 1999, edited by M. H. Manghnani, W. J. Nellis, and M. F. Nicol (Universities Press, Hyderabad, India, 2000), p. 443.

⁵J. P. Perdew, K. Burke, and M. Ernzerhof, *Phys. Rev. Lett.* **77**, 3865 (1996).

⁶P. E. Blöchl, *Phys. Rev. B* **50**, 17953 (1994); G. Kresse and D. Joubert, *ibid.* **59**, 1758 (1999).

⁷The plane-wave cutoff energy is 66.15 Ry, and an unshifted $50 \times 50 \times 50$ uniform mesh is used for the k -point sampling, result-

ing in 3276 and 11076 k points in the irreducible Brillouin zone for the bcc and rhombohedral lattices, respectively. For all of the calculations we use a two-atom supercell that corresponds to the unit cube in the case of the bcc structure. PAW potentials with 13 valence electrons ($3s$, $3p$, $3d$, and $4s$ states) are used.

⁸M. Dacorogna, J. Ashkenazi, and M. Peter, *Phys. Rev. B* **26**, 1527 (1982).

⁹I. M. Lifshitz, *Sov. Phys. JETP* **11**, 1130 (1960).

¹⁰Full-potential linear muffin-tin orbital (FP-LMTO) method, J. M. Wills *et al.*, in *Electronic Structure and Physical Properties of Solids: The Uses of the LMTO Method*, edited by H. Dreysse, *Lecture Notes in Physics* (Springer, Berlin, 2000) pp. 148–167.

¹¹J. D. Greiner, O. N. Carlson, and J. F. Smith, *J. Appl. Phys.* **50**, 4394 (1979); E. S. Fisher and J. F. Remark, *ibid.* **51**, 927 (1980).

¹²J. E. Klepeis and P. Söderlind (to be published).

¹³A. K. McMahan, *Physica B & C* **139&140**, 31 (1986).

¹⁴M. J. Mehl, A. Aguayo, L. L. Boyer, and R. de Coss, *Phys. Rev. B* **70**, 014105 (2004).